

Sensor and Simulation Notes

Note 258

June 1979

THE SINGULARITY EXPANSION METHOD APPLIED TO
PERPENDICULAR CROSSED WIRES OVER A PERFECTLY
CONDUCTING GROUND PLANE

By

Terry T. Crow
Clayborne D. Taylor
Murali Kumbale

CLEARED
FOR PUBLIC RELEASE
PLIPA 5/15/87

ABSTRACT

The singularity expansion method (SEM) has been applied to determine natural resonances of a set of perpendicular crossed wires over a perfectly conducting ground plane. The variation of the natural resonances and the mode and coupling vectors have been studied as parameters of the system varied.

This work was supported by the U. S. Air Force Office of Scientific Research through Grant AFOSR-77-3342.

PL 96-1129

I. INTRODUCTION

Using the singularity expansion method (SEM) one can determine the time domain scattering characteristics of a conducting object in terms of a summation of damped sinusoids [1]. In the evaluation of the SEM solutions the natural resonances or frequencies of the scattering object must be calculated. Here SEM is applied to a study of perpendicular crossed wires over a perfectly conducting ground plane. The results are of interest for at least three reasons: 1) the SEM solution provides insight into the EMP interaction of an aircraft with a ground plane, 2) SEM can be used with success for reasonably complicated geometries (compared to single cylinders) over ground planes, 3) the resonances are located using the Cauchy integral theorem which definitely enhances the usefulness of SEM [2].

This paper is the sequel to an earlier paper co-authored by two of the present authors [3]. The previous paper considered the crossed wire configuration in free space.

II. FORMULATION

In this study the exact field expressions [4] for both axial and radial components are used in conjunction with a sinusoidal current expansion to derive a system of linear equations of the following form [3]

$$\bar{Z}(s) \bar{J}(s) = \bar{E}(s) \quad (1)$$

where $\bar{Z}(s)$ is the square system matrix, $\bar{J}(s)$ is a column matrix whose elements are the unknown current expansion coefficients, and $\bar{E}(s)$ is a column matrix whose elements are particular values of the incident field components.

The SEM problem described herein is formulated in exactly the same manner as that described by Crow, Graves, and Taylor [3]. The following considerations are made in addition to the previous ones:

1. The free space equations are modified to account for image currents parallel to the ground plane having image currents antiparallel to the object currents.
2. If one is interested in the actual calculation of currents and charges, the ground reflected wave must be included in the excitation terms.
3. The King-Wu junction conditions [5] are imposed at the junction of the crossed wires. For n wires at a junction

$$q_1 \psi_1 = q_2 \psi_2 = \dots = q_n \psi_n$$

where q_i is the charge per unit length on the conductor i , radius a_i , and $\psi_i = 2[\ln(2/ka_i) - \gamma]$, $\gamma = 0.5772$.

4. The Kirchhoff current law is enforced at the junction.

The equations and techniques of SEM are well-documented [e.g. 1,3] so they will not be repeated. In earlier studies, the natural frequencies of the scatterers were located by numerical routines based on either a Newton-Raphson technique [6] or a Muller iteration scheme [7]. In this study an algorithm based on the Cauchy integral theorem [2] is used to locate the natural resonances of the scatterer. The greatest advantage of this technique is that one does not have to make initial guesses for the natural frequencies (zeros of the determinant of the system matrix) nor worry about the rate at which the functions approach their zeros (e.g. in the Muller routine it is easy to miss a zero as one moves about in the complex s -plane if the resonance is very narrow).

The basic ideas of this zero search routine can be outlined as follows. Assume there exists a meromorphic function $f(s)$ in a domain D bounded by a

contour C such that no poles or zeros of $f(s)$ lie on the contour. Also assume $f(s)$ has only first order poles and zeros: it follows that

$$\frac{1}{2\pi j} \oint_C \frac{f'(s)}{f(s)} ds = N_o - N_p \quad (2)$$

where $N_o(N_p)$ is the number of zeros (poles) of f with respect to s contained within C. If there are no poles within C, then (2) can be used to determine N_o . Next one forms the equations

$$I_k = \frac{1}{2\pi j} \oint_C s^k \frac{f'(s)}{f(s)} ds = s_1^k + s_2^k + \dots + s_{N_o}^k \quad (3)$$

$k = 1, 2, 3, \dots, N_o$

where s_i is the location of the i th zero in the complex plane. Evaluating the I_k 's by means of Gaussian quadrature along a chosen path C, one has a set of N_o equations for the N_o unknowns.

III. RESULTS AND CONCLUSIONS

The basic geometry of the system being considered is shown in figure 1. In table 1 five sets of the first six natural frequencies are given for reference. The mode designation is based on the required excitation symmetry with respect to the yz plane (symmetric or asymmetric), number of half wavelengths per linear element ($n = 1, 2, 3$, etc.) and multipole moment of the current mode (dipole $n' = 1$, quadrupole $n' = 2$, etc.). The rationale for this designation is given by Baum et al. [11]. Note that for the antisymmetric modes there is no current on wire no. 1. The singularities $s_{as,1}$ and $s_{as,3}$ have been calculated independently by Shumpert and Galloway [8] using a different numerical method. Figure 2 exhibits the variation of the natural frequencies as the height, h , above the ground plane varies.

As has been so dramatically illustrated in previous work [9], the trajectories of the singularities become complicated and, in some cases, difficult to follow as h varies. Due to time limitations, the trajectory of $s_{sy,3,1}$ has been stopped at $h/L = 0.33$. Here it is noted that the real parts of the natural frequencies decrease significantly as the wire configuration approaches the ground. This indicates that the Q 's of the natural resonances increase as the wires approach the ground. Also shown in figure 2 are six natural frequencies calculated using a transmission line approximation [10] - the real parts of the natural frequencies for the transmission line formulation vanish for the perfectly conducting ground case.

Figure 3 shows the variation in the natural frequencies as all variables remain the same as the reference case ($\ell'_1 + \ell_1 = 2\ell_2 = L$, $a_1 = a_2$, $L/a_2 = 20$, $h/L = .2$) except the crossing point (ℓ'_1/ℓ_1) of the two cylinders varies.

As would be expected the locations of the resonances $s_{as,1}$ and $s_{as,3}$ are unaffected by this change. Figure 4 results are for the reference case ($\ell'_1/\ell_1 = 0.5$) but the length of the "y-wire" varies such that $2\ell_2/(\ell'_1 + \ell_1)$ varies. Again, since $2\ell_2$ is held constant, it is reasonable to expect that $s_{as,1}$ and $s_{as,3}$ remain constant. Figure 5 traces the resonance trajectories as the radius of the elements varies from the reference case.

Figures 6 through 8 are plots of the real components of the natural current modes for the crossed wire structure above the ground plane. (In figure 7 the mode vector on the negative y-wire is very small compared to the elements shown but not identically zero.)

IV. THE EXCITATION VECTOR AND CURRENT CALCULATIONS

The excitation vector is defined in terms of one of the two polarizations shown in figure 9. In the x,y plane, the incident fields are

$$\vec{E}_1^i = [\hat{i}_x E_1 \cos(\phi_i + \pi/2) + \hat{i}_y E_1 \sin(\phi_i + \pi/2)] \cdot \exp \gamma [ct + x \sin \theta_i \cos \phi_i + y \sin \theta_i \sin \phi_i + z \cos \theta_i] \quad (4)$$

$$\vec{E}_2^i = [\hat{i}_x E_2 \sin(\pi/2 - \theta_i) \cos \phi_i + \hat{i}_y E_2 \sin(\pi/2 - \theta_i) \sin \phi_i] \cdot \exp \gamma [ct + x \sin \theta_i \cos \phi_i + y \sin \theta_i \sin \phi_i + z \cos \theta_i] \quad (5)$$

while the ground reflected waves are

$$\vec{E}_1^r = [-\hat{i}_x E_1 \cos(\phi_i + \pi/2) - \hat{i}_y E_1 \sin(\phi_i + \pi/2)] \cdot \exp \gamma [ct + x \sin \theta_i \cos \phi_i + y \sin \theta_i \sin \phi_i - z \cos \theta_i] \quad (6)$$

$$\vec{E}_2^r = [-\hat{i}_x E_2 \sin(\pi/2 - \theta_i) \cos \phi_i - \hat{i}_y E_2 \sin(\pi/2 - \theta_i) \sin \phi_i] \cdot \exp \gamma [ct + x \sin \theta_i \cos \phi_i + y \sin \theta_i \sin \phi_i - z \cos \theta_i] \quad (7)$$

where $\gamma = \frac{s}{c} = \frac{\sigma}{c} + j \left(\frac{\omega}{c} = k\right)$. For example, E_1 polarization with $\phi_i = 0$,

$\theta_i = 0$, the total excitation vector, $\vec{E}_1^T = \vec{E}_1^i + \vec{E}_1^r$, becomes at $z = h$

$$\vec{E}_1^T = \hat{i}_y E_1 e^{\gamma[ct + h]} [1 - e^{-2\gamma h}]$$

It is convenient to define $x_m = \max |x \sin \theta_i \cos \phi_i|$ and $y_m = \max |y \sin \theta_i \sin \phi_i|$, and $q = \max \{x_m \text{ or } y_m\}$. If t' is defined such that $t' = 0$ when the incident wave first strikes a point on the structure, then

$$t = t' - \frac{q + h \cos \theta_i}{c}$$

The incident wave is multiplied by the unit Heaviside function

$$u_i [ct' - q + x \sin \theta_i \cos \phi_i + y \sin \theta_i \sin \phi_i] \quad (8)$$

and the reflected wave by

$$u_r [ct' - q - 2h \cos \theta_i + x \sin \theta_i \cos \phi_i + y \sin \theta_i \sin \phi_i] \quad (9)$$

where $u(\ell) = 1 \quad \ell \geq 0$

$$= 0 \quad \ell < 0.$$

With a notation similar to that of Umashankar et al [9], the current

expression becomes

$$\bar{i}(t) = \sum_i \beta_i \frac{\bar{M}_i \bar{C}_i^T}{s_i} [\bar{E}^i u(\tau_1) e^{s_i \tau_1 / c} - \bar{E}^r u(\tau_2) e^{s_i \tau_2 / c}] \quad (10)$$

$$\tau_1 = ct' - q + x \sin \theta_i \cos \phi_i + y \sin \theta_i \sin \phi_i$$

$$\tau_2 = ct' - q - 2h \cos \theta_i + x \sin \theta_i \cos \phi_i + y \sin \theta_i \sin \phi_i$$

$\bar{E}_{i,r}$ are column vectors; the elements of these vectors are the appropriate tangential field terms evaluated from the first square brackets of equations (4) - (7): e.g. if element number 1 of the mode vector represents the zone on wire 2 nearest the intersection point on the negative x-axis, it follows that the first element of the E vectors will be the x-component of the corresponding field expression. Figure 10 shows the results of one such current calculation for junction currents for E_1 polarization, $\theta = 0^\circ$, $\phi = 0^\circ$, and the incident wave is the unit step where E_1 or $E_2 = 1$ v/m.

Several comments are in order concerning the placement of the Heaviside function in the expression for the current (10). As (10) is written each entry in the excitation matrix \bar{E} is multiplied by a Heaviside function. As soon as one Heaviside function becomes non-zero, the current at every point on the structure becomes non-zero (unless of course \bar{M}_i has some zero entries) for a particular s_i . Since causality is a part of the original theory, it follows that the sum of i in (10) should lead to zero currents at appropriate places and times if one considers all natural resonances. In practice however one normally sums over only four to ten or so terms, and numerically it appears causality is lost. Causality can be preserved by moving the Heaviside function from the excitation matrix to the mode vector matrix but in this case the product $\bar{C}_i^T \bar{E}$ is calculated as though all zones are excited simultaneously and

the arrival times of the incident wave(s) are ignored. These problems are not unique to our problems but have existed from the beginning of SEM [6].

to be considered

REFERENCES

1. C. E. Baum, "The Singularity Expansion Method," in Transient Electromagnetic Fields, Topics in Applied Physics, Vol. 10, 1976 (Editor, L. B. Felsen).
2. B. K. Singaraju, D. V. Giri, and C. E. Baum, "Further developments in the evaluation of the zeros of analytic functions and relevant computer programs," Math Note 42, Air Force Weapons Laboratory, Kirtland AFB, NM, March 1976.
3. T. T. Crow, B. D. Graves, and C. D. Taylor, "The singularity expansion method as applied to perpendicular crossed wires," IEEE Trans. Antennas Propagat., vol. AP-23, pp. 540-546, July 1975. See also "The singularity expansion method as applied to perpendicular crossed cylinders in free space", IN 161, Air Force Weapons Laboratory, Kirtland AFB, NM, Oct. 1973 (same authors).
4. S. A. Schelkunoff and H. T. Friis, Antennas: Theory and Practice. New York: Wiley, 1952, p. 370.
5. T. T. Wu and R. W. P. King, "The tapered antenna and its application to the junction problem for thin wires," IEEE Trans. Antennas Propagat., vol. AP-24, pp. 42-46, Jan. 1976. Also IN269, Jan. 1976.
6. F. M. Tesche, "On the analysis of scattering and antenna problems using the singularity expansion techniques," IEEE Trans. Antennas Propagat., vol. AP-21, pp. 53-62, Jan. 1973. See also "On the singularity expansion method as applied to electromagnetic scattering from thin wires", IN 102, Air Force Weapons Laboratory, Kirtland AFB, NM, Apr. 1972 (same author).
7. T. T. Crow, B. D. Graves, and C. D. Taylor, "Numerical techniques useful in the singularity expansion method as applied to electromagnetic interaction problems," Math Note 27, Air Force Weapons Laboratory, Kirtland AFB, NM, Dec. 1972.
8. T. H. Shumpert and D. J. Galloway, "Finite Length Cylindrical Scatterer Near Perfectly Conducting Ground - A Transmission Line Mode Approximation," IEEE Trans. Antennas Propagat., vol. AP-26, pp. 145-151, Jan. 1978. See also "Transient analysis of a finite length cylindrical scatterer very near a perfectly conducting ground," SSN 226, Air Force Weapons Laboratory, Kirtland AFB, NM, August 1976 (same authors).
9. K. R. Umashankar, T. H. Shumpert, and D. R. Wilton, "Scattering by a Thin Wire Parallel to a Ground Plane Using the Singularity Expansion Method," IEEE Trans. Antennas Propagat., vol. AP-23, pp. 178-184, March 1975. See also T. H. Shumpert, "EMP interaction with a thin cylinder above a ground plane using the singularity expansion method," IN 182, Air Force Weapons Laboratory, Kirtland AFB, NM, June 1973; and K. R. Umashankar and D. R. Wilton,

"Transient scattering by a thin wire in free space and above ground plane using the singularity expansion method," IN 236, Air Force Weapons Laboratory, Kirtland AFB, NM, August 1974.

10. C. D. Taylor and V. D. Naik, "An Analytical Singularity Expansion Method Solution for Wires in Proximity to a Perfect Ground." presented at the IEEE/P-S, URSI 1978 Spring meeting, Washington, D. C. See also C. D. Taylor, V. D. Naik, and T. T. Crow, "A study of the EMP interaction with aircraft over an imperfect ground plane - a transmission line theory approximation." To be published as a Sensor and Simulation Note.
11. C. E. Baum, C. D. Taylor and T. T. Crow, "On the Designation of Natural Modes for Certain Thin-Wire Structures." To be published as an Interaction Note.

resonance	sL/C		sL/C	
	free space, this study	free space [4]	free space [8]	
			approx.	exact
sy,1,1	-0.2923 + j 2.319	-0.2935 + j 2.292		
as,1	-0.4242 + j 2.503	-0.4203 + j 2.508	-0.4279 + j 2.5377	-0.4380 + j 2.5847
sy,1,2	-0.3426 + j 3.726	-0.3346 + j 3.839		
sy,2,2	-0.6786 + j 6.066	-0.6609 + j 6.066		
sy,3,1	-1.0166 + j 8.139	-1.0065 + j 8.156		
as,3	-0.9852 + j 8.305	-0.9528 + j 8.294	-0.8167 + j 8.1833	-0.7866 + j 8.4120
	h/L = 0.2 this study		h/L = 0.2 [8]	
			approx.	exact
sy,1,1	-0.0513 + j 2.361			
as,1	-0.0898 + j 2.592		-0.091 + j 2.617	-0.1085 + j 2.611
sy,1,2	-0.1021 + j 3.769			
sy,2,2	-0.3909 + j 5.740			
sy,3,1	-0.6691 + j 7.581			
as,3	-0.6478 + j 8.034			

Table 1. Natural frequencies for a crossed wire structure.

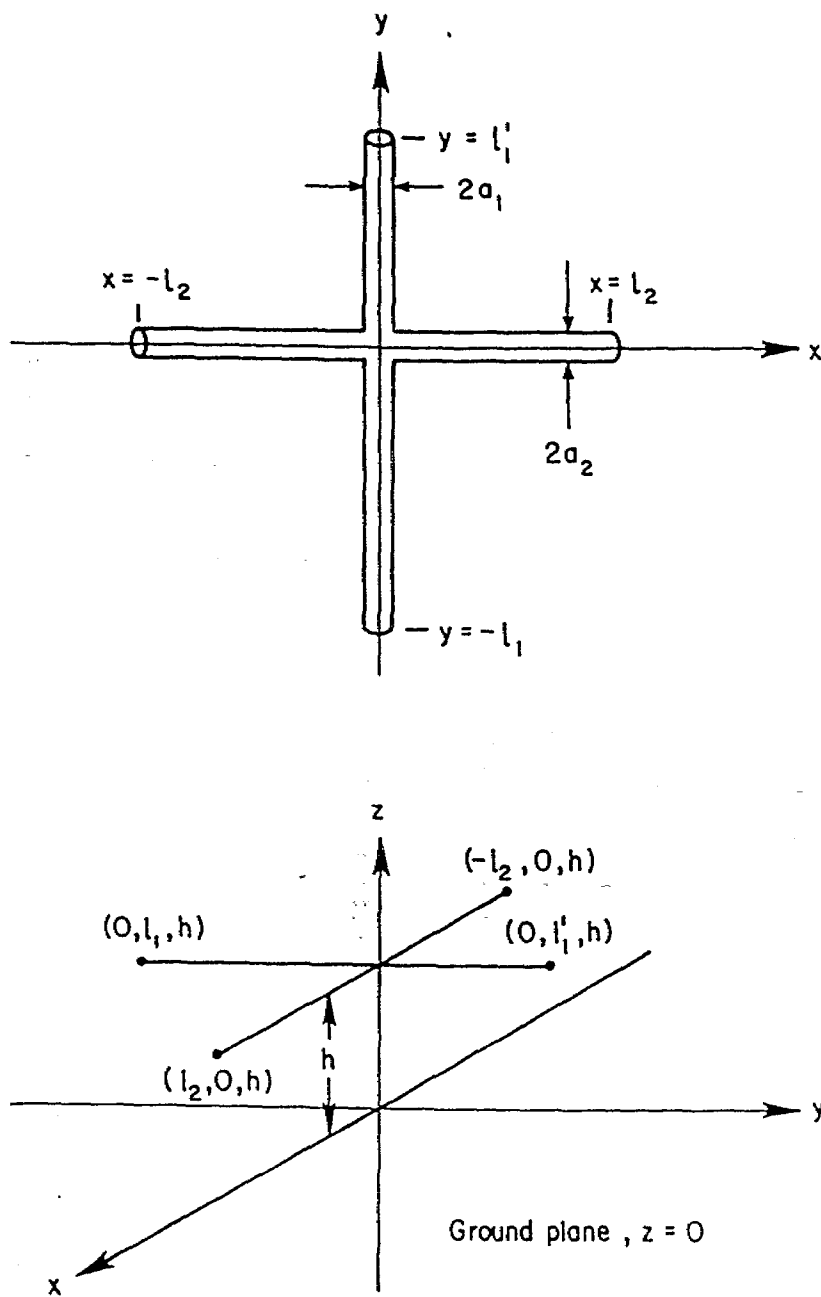


Figure 1. The crossed wire configuration over a perfectly conducting ground plane.

- Real Component (Right Scale)
- Imaginary Component (Left Scale)
- Imaginary Components from Transmission Line Theory

$$\ell'_1/\ell_1 = 0.5, L = \ell'_1 + \ell_1 = 2\ell_2, a_1 = a_2, L/a_2 = 20$$

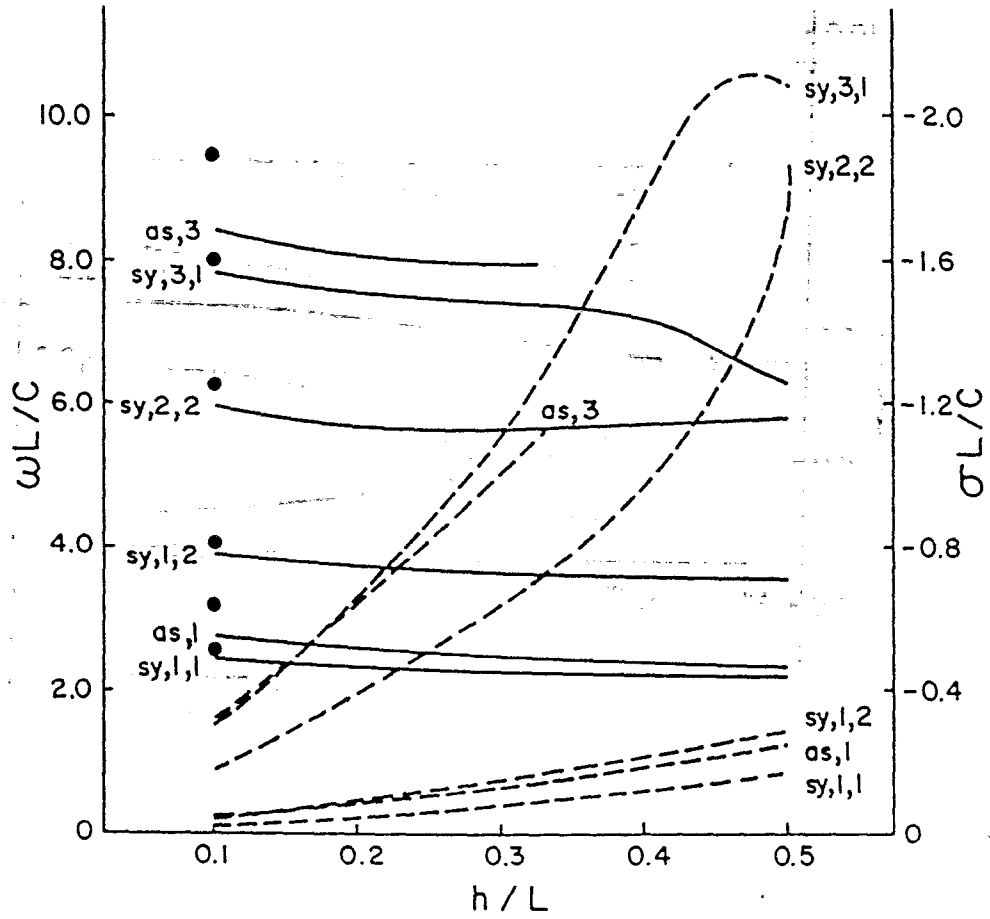


Figure 2: Variation of the natural frequencies with change in height of the crossed wires over a perfect ground.

--- Real Component (Right Scale)
 —— Imaginary Component (Left Scale)

$$L = 2\ell_2 = \ell_1' + \ell_1, \quad a_1 = a_2, \quad L/a_2 = 20, \quad h/L = 0.2$$

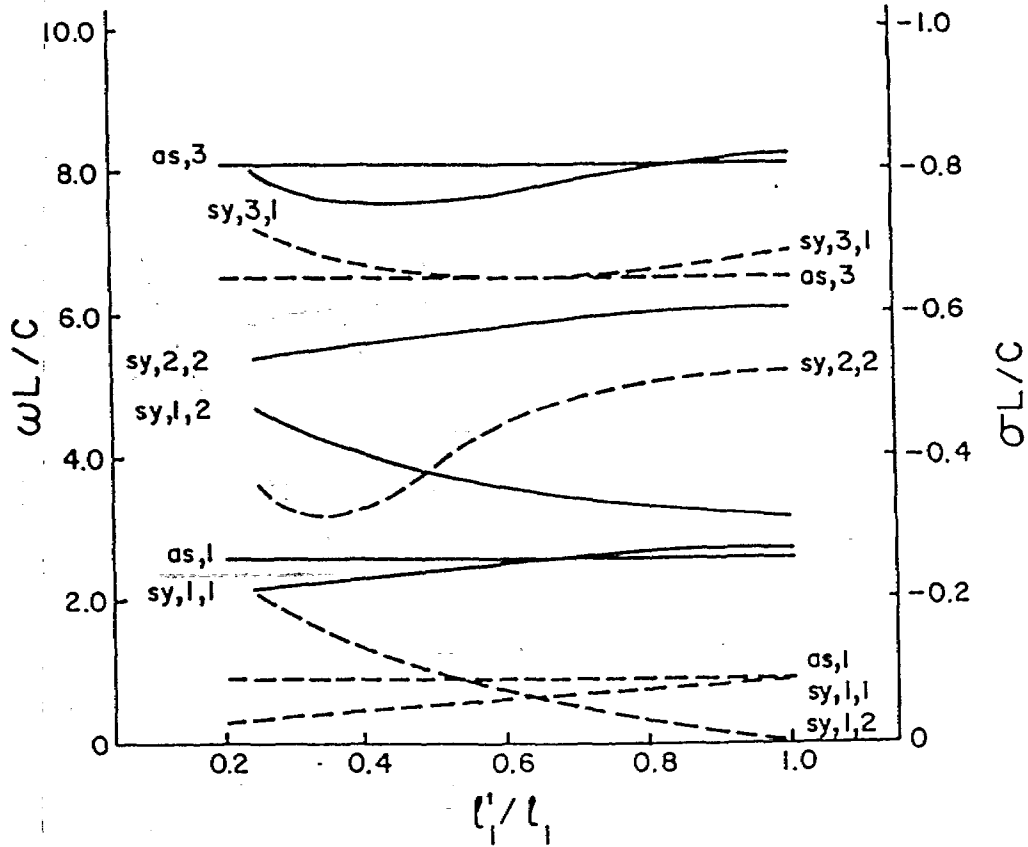


Figure 3: Variation of the natural frequencies with change in crossing point for crossed wires over a perfect ground.

----- Real Component (Right Scale)

———— Imaginary Component (Left Scale)

$$L = 2l_2, \quad l_1'/l_1 = 0.5, \quad a_1 = a_2, \quad L/a_2 = 20, \quad h/L = 0.2$$

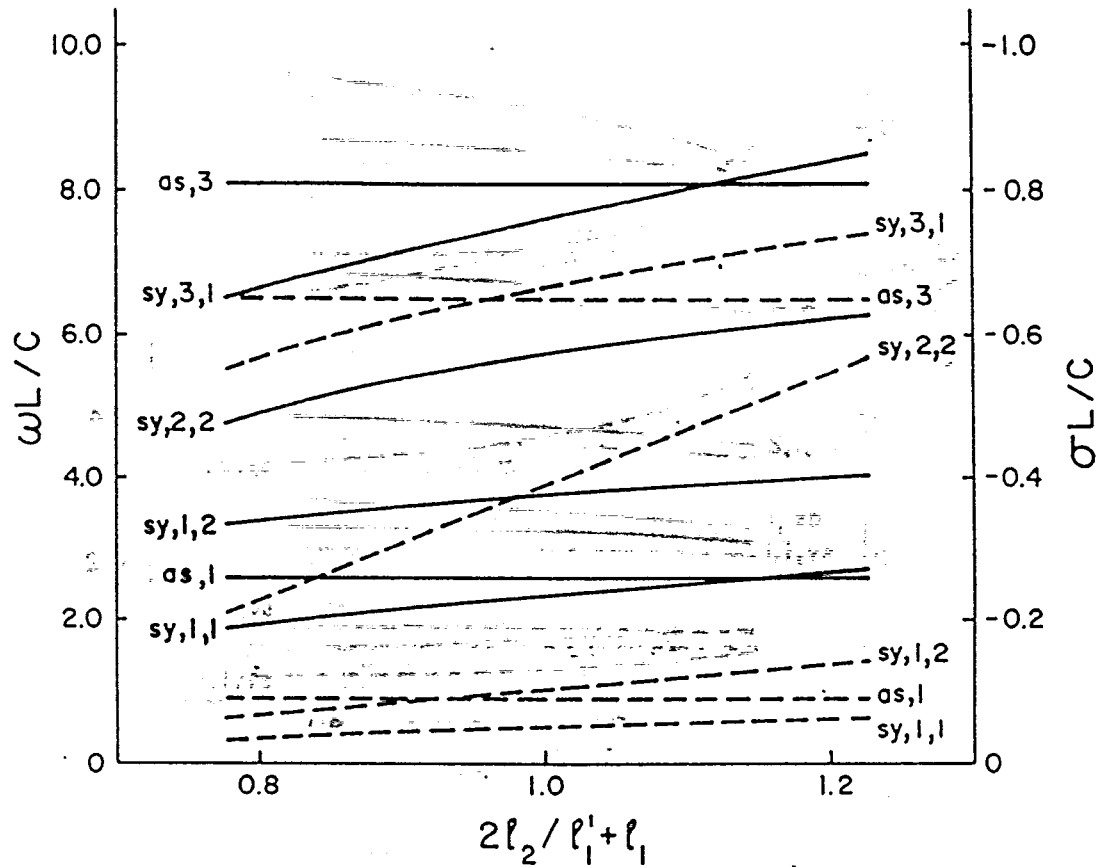


Figure 4: Variation in the natural frequencies with change in relative wire lengths for crossed wires over a perfect ground.

----- Real Component (Right Scale)

———— Imaginary Component (Left Scale)

$$L = 2l_2 = l_1' + l_1, \quad l_1'/l_1 = 0.5, \quad a_1 = a_2, \quad h/L = 0.2$$

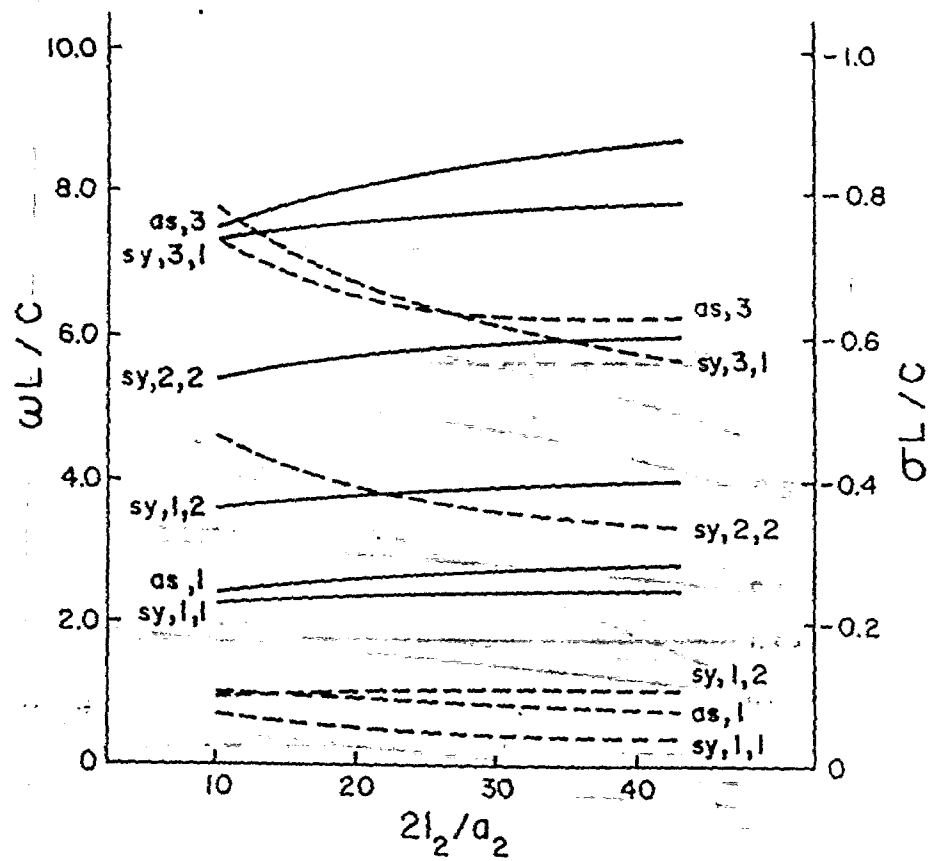


Figure 5: Variation in the natural frequencies with change in wire radius for crossed wires over a perfect ground.

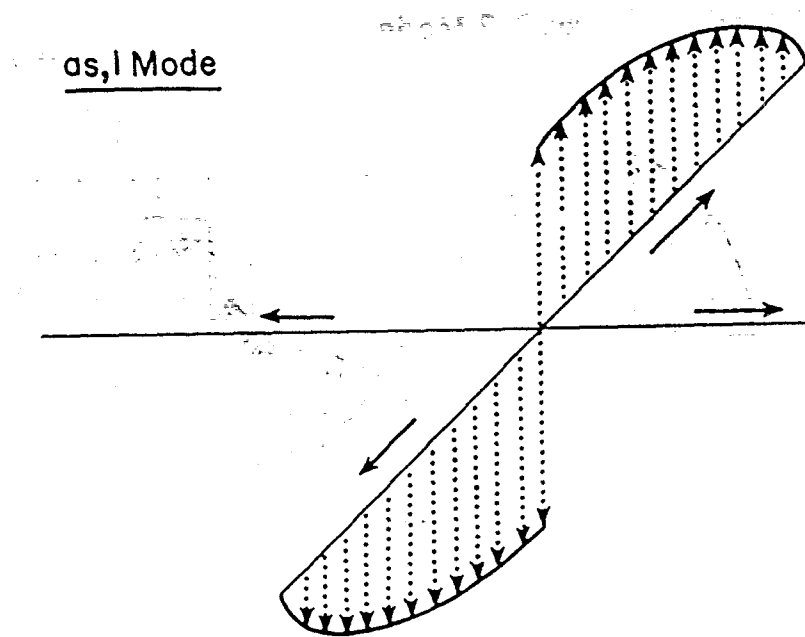
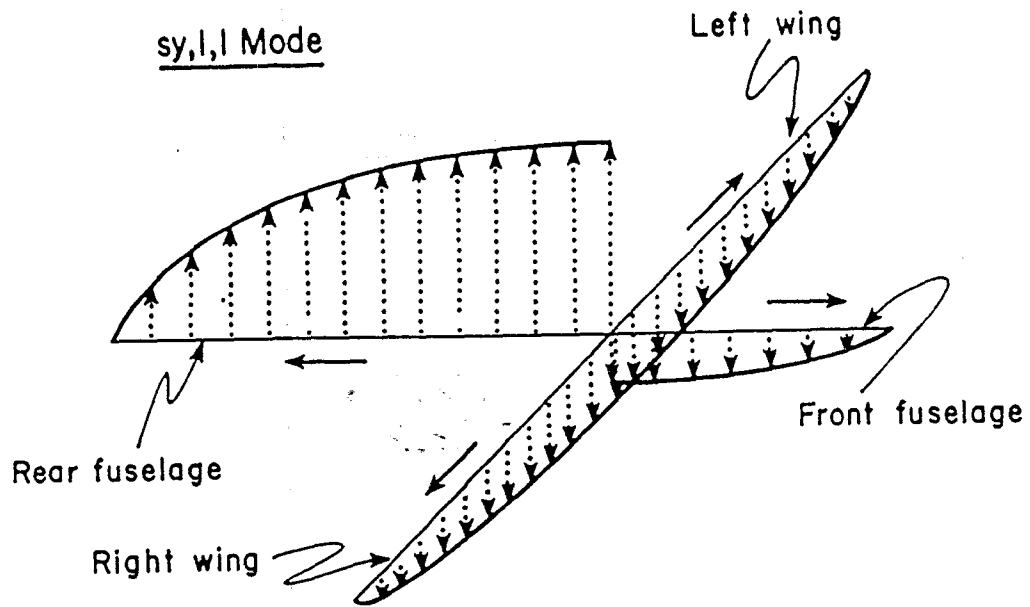


Figure 6: The $sy,1,1$ and the $as,1$ natural current modes a crossed wire structure over a ground plane.
 $\ell_1' = \ell_1/2$, $h = .1L$, $L = 2\ell_2 = \ell_1' + \ell_1$,
 $a_1 = a_2 = L/20$. Arrows indicate directions assumed for positive current.

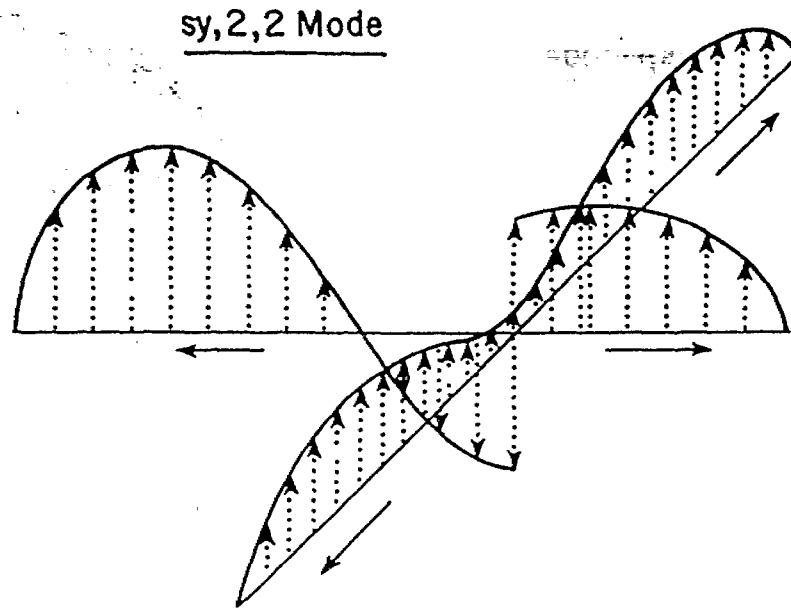
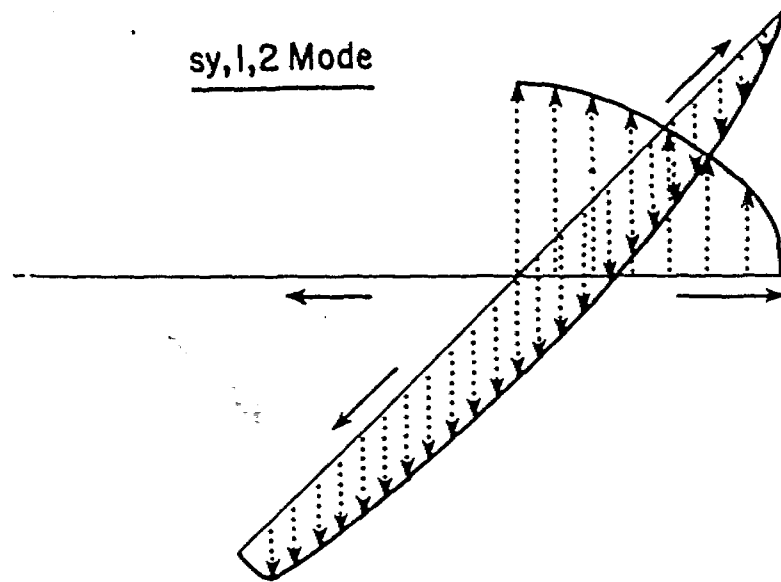
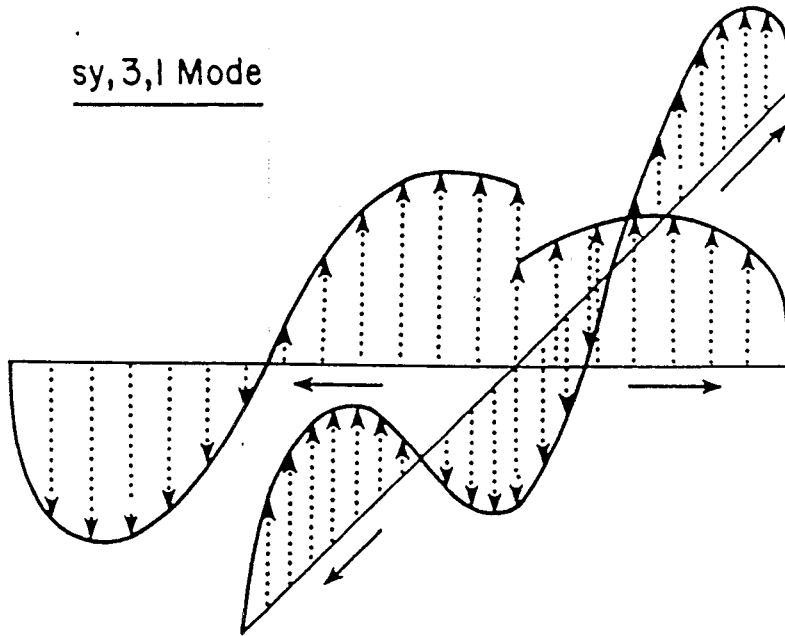


Figure 7: The $sy,1,2$, and the $sy,2,2$ natural current modes for a crossed wire structure over a ground plane.
 $l_1' = l_1/2$, $h = .1L$, $L = 2l_2 = l_1' + l_1$,
 $a_1 = a_2 = L/20$. Arrows indicate directions assumed for positive current.

sy, 3, 1 Mode



as, 3 Mode

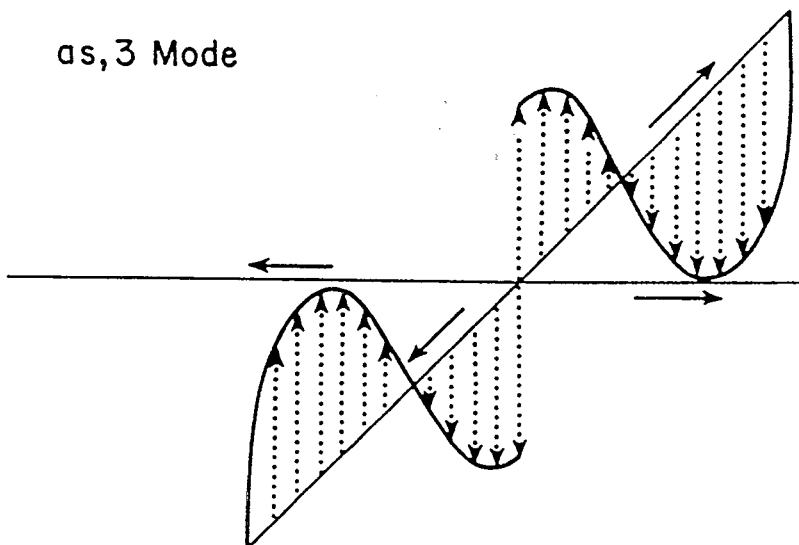


Figure 8: The sy, 3, 1 and the as, 3 natural current modes for a crossed wire structure over a ground plane.
 $\ell_1' = \ell_1/2$, $h = .1L$, $L = 2\ell_2 = \ell_1' + \ell_1$,
 $a_1 = a_2 = L/20$. Arrows indicate directions assumed for positive current.

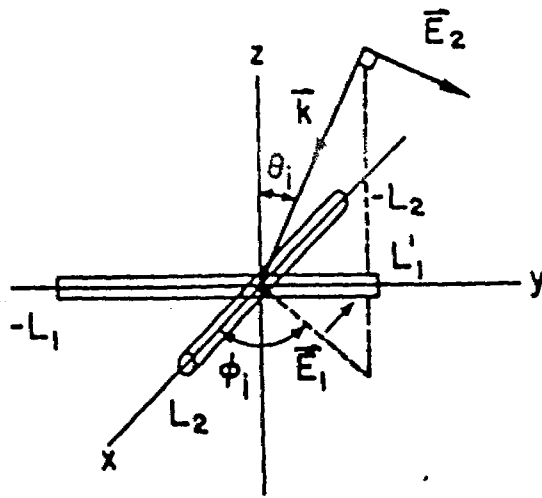


Figure 9: Incident field angles and polarizations.

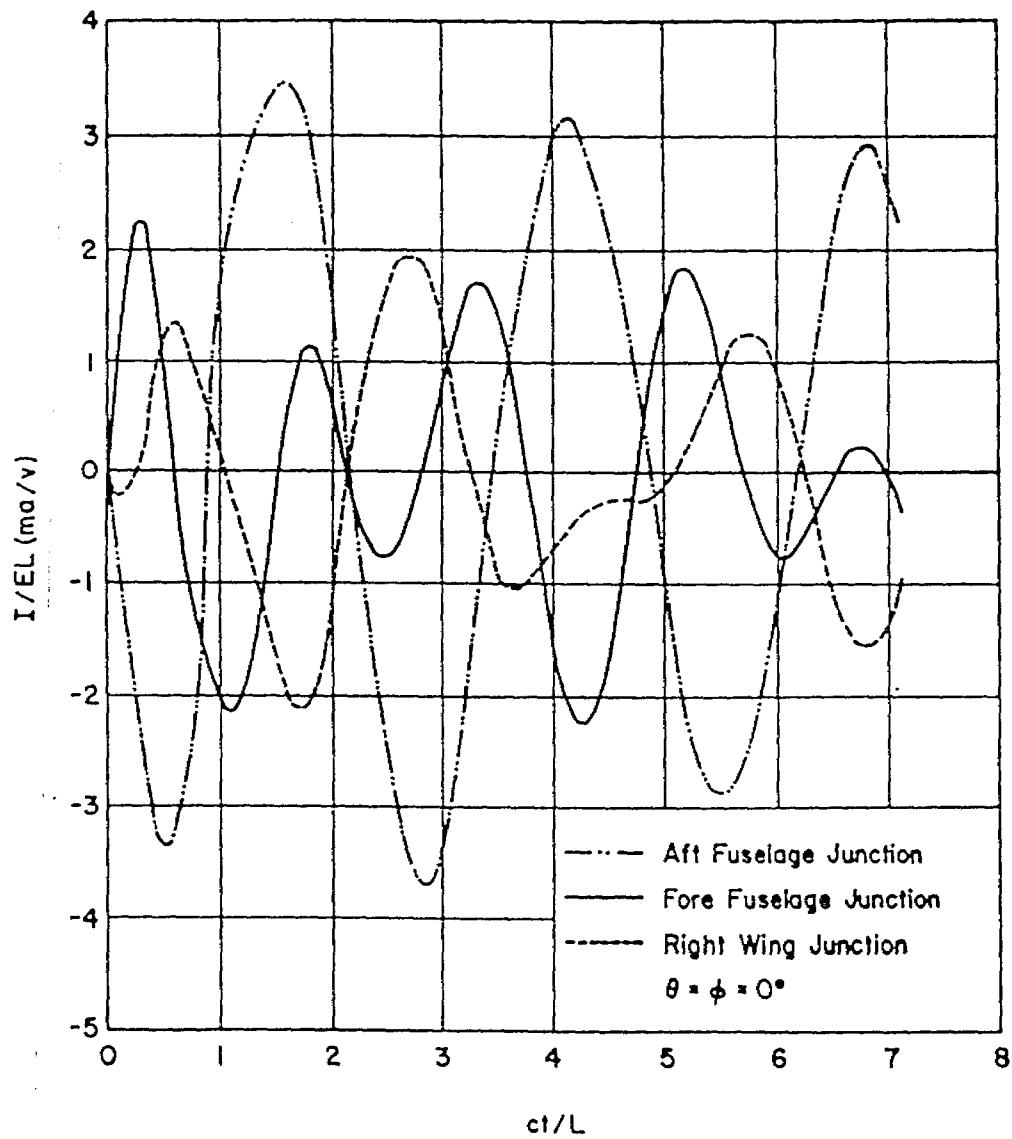


Figure 10: Junction currents versus time for a normally incident plane wave.